Analyst

CRITICAL REVIEW

Cite this: *Analyst*, 2017, **142**, 2862

A road map for multi-way calibration models

Graciela M. Escandar * and Alejandro C. Olivieri *

A large number of experimental applications of multi-way calibration are known, and a variety of chemometric models are available for the processing of multi-way data. While the main focus has been directed towards three-way data, due to the availability of various instrumental matrix measurements, a growing number of reports are being produced on order signals of increasing complexity. The purpose of this review is to present a general scheme for selecting the appropriate data processing model, according to the properties exhibited by the multi-way data. In spite of the complexity of the multi-way instrumental measurements, simple criteria can be proposed for model selection, based on the presence and number of the so-called multi-linearity breaking modes (instrumental modes that break the low-rank multi-linearity of the multi-way arrays), and also on the existence of mutually dependent instrumental modes. Recent literature reports on multi-way calibration are reviewed, with emphasis on the models that were selected for data processing.

Received 17th May 2017,
Accepted 27th June 2017

DOI: 10.1039/c7an00822h

rsc.li/analyst

Introduction

Multi-way calibration carries the potentiality of realizing the dream of analytical chemistry,[1,2] because: (1) the second-order advantage can be achieved: analytes can be quantitated in the presence of uncalibrated interferents,[3,4] (2) only small, pure-analyte calibration sets are needed, instead of large calibration sets containing all possible interferents (as required by first-order multivariate calibration), (3) sample clean-up steps may no longer be needed, (4) full chromatographic resolution is not required and separation experiments are shorter and simpler,[5] and (5) the selectivity and sensitivity increase as the number of instrumental modes increases.[6]

Departamento de Química Analítica, Facultad de Ciencias Bioquímicas y Farmacéuticas, Universidad Nacional de Rosario, Instituto de Química de Rosario (IQUIR-CONICET), Suipacha 531, Rosario S2002LRK, Argentina.
E-mail: escandar@iquir-conicet.gov.ar, olivieri@iquir-conicet.gov.ar

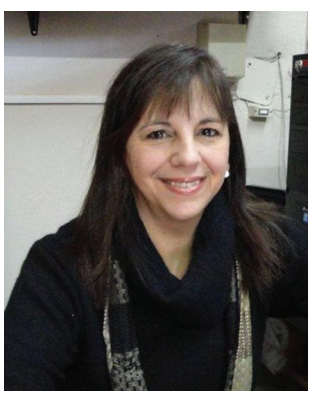

Graciela M. Escandar

Graciela Escandar was born in Rosario, Argentina. She obtained her B. Sc. degree in Biochemistry in 1983 and her Ph. D. in 1992, both from the Faculty of Biochemical and Pharmaceutical Sciences, University of Rosario, where she is now Associate Professor in the Department of Analytical Chemistry, and a fellow of the National Research Council of Argentina (CONICET). She has published more than 100 scientific papers in international journals, a book and book chapters, and supervised seven Ph.D. theses. Her research focuses on the development of new luminescence methodologies coupled to multi-way calibration of analytes of environmental and pharmaceutical interest.

Alejandro C. Olivieri

Alejandro Olivieri was born in Rosario, Argentina, on July 28, 1958. He obtained his B.Sc. degree in Industrial Chemistry from the Catholic Faculty of Chemistry and Engineering in 1982, and his Ph.D. from the Faculty of Biochemical and Pharmaceutical Sciences, University of Rosario in 1986. He currently works in the Department of Analytical Chemistry of the latter Faculty, and is a fellow of the National Research Council of Argentina (CONICET). He has published about 200 scientific papers in international journals, several books and book chapters and supervised ten Ph.D. theses. He was a John Simon Guggenheim Memorial Foundation fellow (2001–2002).

It is important to first define the term 'mode', a specific expression relevant to multi-way calibration which will be referred to in the remainder of this work. When measuring complex instrumental data, a mathematical object can be built with the collected multi-way data array. The number of instrumental modes is the number of directions in the multi-dimensional space spanned by the latter array.

Many different multi-way mathematical models have been described in the literature, and model selection often puzzles the analyst. In this context, it is important to have a unified scheme which would allow one to select a data processing model in a rational manner. This requires some knowledge on the relationship between model features and data properties. As we shall see, the latter greatly depend on the mutual relationship among the profiles describing the behavior of sample constituents in various data modes.

Multi-way calibration has been compiled in recent books,[1,2] and also in several literature reviews.[4,5–9] New developments in both the theory and application of multi-way calibration make the present review timely. We have organized it in two major blocks: (1) a description of various multi-way data types and the models which should in principle be employed for data processing according to the data properties, and (2) a discussion of recent literature reports on second- and third-order experimental calibration (three- and four-way). The primary experimental examples to be described involve excitation–emission fluorescence matrices (EEFM) and chromatography with spectral detection, although various other sources of multi-way signals are gradually appearing in the scene.

Data classification and model selection

Second-order/three-way data and models

We first recall the distinction between order and ways: the order is the number of modes of the data array measured for a single sample, whereas the number of ways is the number of modes of an array which can be built with data for a sample set. Thus, first-order and two-way calibration are synonymous, as are second-order and three-way, third-order and four-way, *etc.*

Second-order data for a group of samples can be arranged into a three-way array with three modes: the sample mode and the two instrumental modes. A key concept for properly classifying these data is whether a constituent profile in a given instrumental mode is constant across samples or not. Sample-dependent modes occur in an important group of experiments, and it is thus critical to be able to identify them for adequate model choice.

In certain experiments, the (normalized) instrumental profiles for all constituents are independent of each other and are also independent of the sample composition. This situation defines a trilinear three-way array, although the correct expression should be low-rank trilinear, meaning that it can be modeled using a small number of components, ideally equal to the number of chemical constituents present in the system.[1] The array can be graphically represented as in Fig. 1A, and the data are adequately modeled by the trilinear equation:

$$x_{ijk} = \sum_{n=1}^{N} a_{in} b_{jn} c_{kn} + e_{ijk} \quad (1)$$

where x_{ijk} is a generic element of the three-way array of signals, a_{in} is proportional to the concentration of constituent n in sample i, b_{jn} is proportional to the profile in one instrumental mode at channel j, c_{kn} is proportional to the profile in the other instrumental mode at channel k and e_{ijk} is the error model. The most popular model for trilinear data is least-squares parallel factor analysis (PARAFAC),[10] because eqn (1) is precisely its defining expression. Other variants are known which attempt to decompose a trilinear three-way array using different strategies, as will be reviewed below.[1]

Another important group of three-way experiments leads to the loss of trilinearity of the three-way array by a number of causes. The most common one is when profiles in one of the instrumental modes are not constant across samples. The sample-dependent mode is responsible for breaking the trilinearity, and is called a trilinearity breaking mode, or a breaking mode in short. These datasets have been classified as non-trilinear type 1.[1] Since these data are not trilinear, eqn (1) cannot be applied. A wise alternative is to unfold the three-way array into a matrix, with one direction defined by the profiles which do not change, and the other one by the concatenation of samples and the breaking mode. The obtained object is

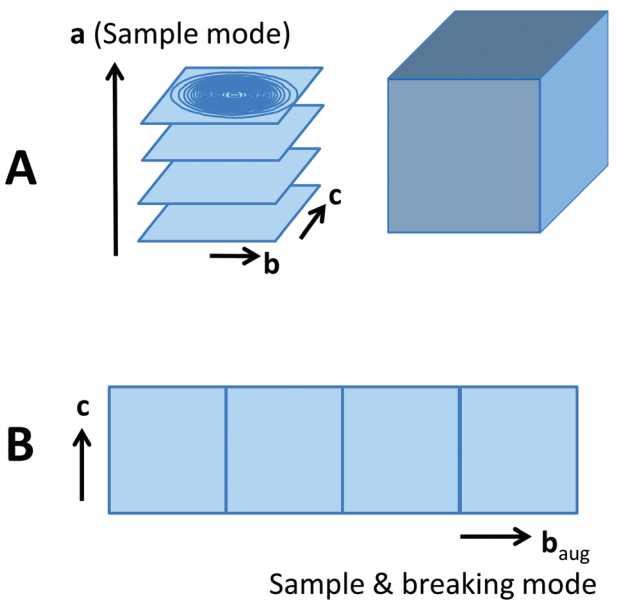

Fig. 1 Graphical illustration of two types of second-order data. (A) Trilinear. A three-way array (right) is built by stacking data matrices (left). The sample mode is represented by **a**, while both instrumental modes are represented by **b** and **c**. (B) Non-trilinear type 1. An augmented data matrix is built by placing individual data matrices for each sample adjacent to each other in the direction of the breaking mode (b_{aug}). The profiles for the other instrumental mode (**c**) are constant across samples.

called an augmented matrix, because it can be thought as being obtained by placing all data matrices adjacent to each other along the direction of the breaking mode (a process called matrix augmentation, represented in Fig. 1B). The matrix is bilinear (more precisely low-rank bilinear) and can be conveniently studied using a bilinear model:[1,11]

$$x_{jk} = \sum_{n=1}^{N} b_{\mathrm{aug},jn} c_{nk} + e_{jk} \quad (2)$$

where x_{jk} is a generic matrix element, $b_{\mathrm{aug},jn}$ is proportional to the concentration profile along the augmented mode (concatenating the sample and breaking modes), c_{nk} is the corresponding profile in the other mode and e_{jk} is an error term. The model of choice here is multivariate curve resolution-alternating least-squares (MCR-ALS) in the so-called extended format,[11] subjected to a number of chemically reasonable constraints during least-squares fit, with a model defining expression which is precisely eqn (2).

Trilinear and non-trilinear type 1 are, by far, the most common three-way data. However, there are additional causes for the loss of trilinearity: both instrumental modes, not depending on each other, may depend on the sample, defining the so-called non-trilinear type 2 data.[1] Data of this type show changes in the profiles in both modes, with specific shapes which depend on the sample composition, and thus vary from sample to sample, defining both modes as breaking,[1] and maintaining the test sample as bilinear. A suitable model for calibrating these data is unfolded partial least-squares with residual bilinearization (U-PLS/RBL), which unfolds all calibration data matrices into vectors, but maintains the test sample in its matrix form to achieve the second-order advantage, because this matrix is low-rank bilinear.

Finally, instrumental profiles may depend on each other, in the sense that constituent profiles along one mode are different for each experimental channel in the other mode, even when they are normalized. These data are called non-trilinear type 3,[1] which may involve further sub-types. Mutually dependent instrumental modes may be independent of the sample, or may be accompanied by a further dependence on samples. The best approach here is apparently to unfold all data matrices into vectors prior to processing. However, very few reports exist in this regard,[12–14] and further work would be necessary to establish the conditions under which the second-order advantage can be achieved from these types of data.

As a summary of the present discussion, the first question to be answered concerns the mutual dependence of the instrumental modes, followed by assessing of the number of trilinearity breaking modes. This helps to properly classify the data and select the model for successful processing.

Third-order/four-way data and models

More complex situations can be found in higher-order systems. When classifying these data and models, focus is again directed to the existence of multi-linearity and to the manners in which multi-linearity may be broken in the presence of breaking and/or dependent modes. In this case, the number of mathematical objects that can be built with the data for a group of samples increases with respect to three-way calibration. The prime candidate is a four-way array, obtained by arranging the data into a four-dimensional object (Fig. 2A). The latter are called quadrilinear, and can be conveniently studied by using a quadrilinear four-way PARAFAC model.[1]

When a single breaking mode occurs, a trilinear three-way array can be built by unfolding the four-way array along the direction defined by the breaking mode. This can also be done by placing the three-way arrays for different samples adjacent to each other in the direction of the breaking mode, leading to an augmented trilinear three-way array (Fig. 2B). These data are non-quadrilinear type 1,[1] and can be modeled using a

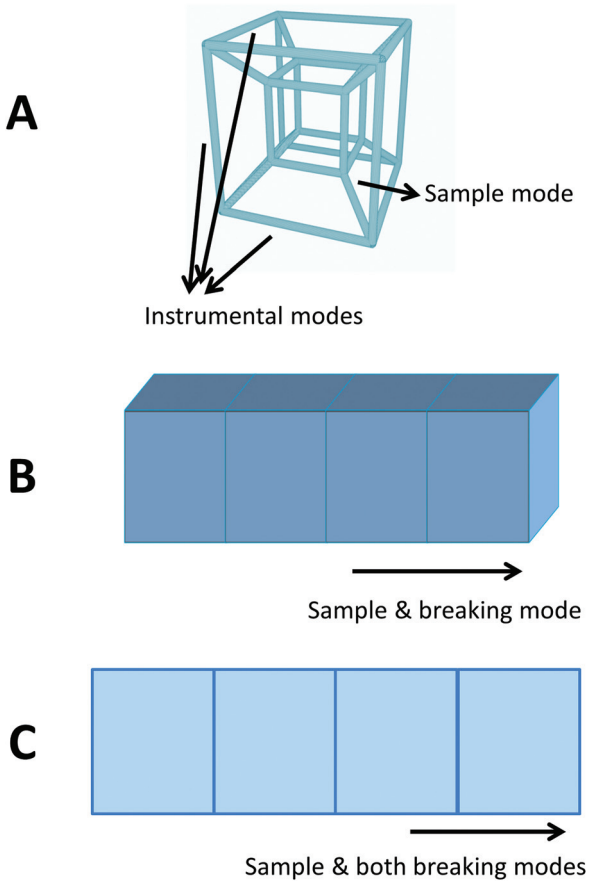

Fig. 2 Graphical illustration of three types of third-order data. (A) Quadrilinear. A four-way array is built with a number of third-order data for a group of samples (the sample and instrumental modes are indicated). (B) Non-quadrilinear type 1. An augmented three-way array is built by placing third-order data for a group of samples adjacent to each other in the direction of the breaking mode. The other instrumental modes are constant across samples. (C) Non-quadrilinear type 2. A super-augmented matrix is built by first concatenating the two instrumental breaking modes for each sample, and then placing the obtained matrices adjacent to each other. The profiles in the remaining instrumental mode are constant across samples.

three-way PARAFAC model, which has been called augmented PARAFAC.[15]

Another case of interest occurs in experiments showing two breaking modes. Here a good alternative is to unfold the four-way array into a matrix, with directions given by the concatenation of the sample and the two breaking modes on one hand, and the additional mode on the other. This can also be imagined to be obtained by first unfolding each three-dimensional array into a matrix, by concatenating the two breaking modes, and then placing each of these matrices adjacent to each other to produce a super-augmented matrix (Fig. 2C). These data are non-quadrilinear type 2.[1] Since the super-augmented matrix is bilinear, it can be successfully processed by extended MCR-ALS.[11]

No systems have been described yet having three breaking modes, which would lead, analogously to second-order/three-way data, to arrays that can be unfolded into vectors, keeping the test sample data in the original three-dimensional fashion for achieving the second-order advantage. These data are non-quadrilinear type 3,[1] and could be tackled by the analogue U-PLS/RTL, *i.e.*, U-PLS with residual trilinearization.[16]

Likewise, no four-way systems have been experimentally produced having instrumental modes depending on each other. They would define non-quadrilinear type 4 data,[1] which would include a number of sub-types, depending on the number of mutually dependent instrumental and sample-depending modes. In the special case where only two modes are mutually dependent, they could be concatenated, producing three-way arrays that could be submitted to the previously discussed analysis of three-way data.

The situation is obviously more complex for fourth-order/five-way data.[17,18] Similar consideration to those discussed above should apply to these datasets.

Experimental examples

Model selection

The above discussion presented the recommendations which should in principle be followed when employing multi-way calibration, *i.e.*, to choose the model which is best suited for the data properties. However, in practical cases, the model of choice differs from these directions, as would be probably confirmed in some of the cases to be reviewed in the next sections. A number of reasons exist for this outcome: (1) trilinear data may require a more flexible model than PARAFAC (*e.g.*, U-PLS/RBL),[19] either because of extensive spectral overlapping or linear dependency among constituent profiles, (2) PARAFAC variants are adapted to the presence of breaking modes, *e.g.* PARAFAC2,[20] whose generality and usefulness in the presence of interferents have been questioned,[21] (3) data were aligned along the breaking mode to produce a trilinear three-way array and subsequently processed by PARAFAC, although this may not be possible, in general, in the presence of interferents,[21] (4) road maps for model selection were not considered. The authors of the present review openly admit to have sometimes fallen in case (4), showing that *the shoemaker's son always goes barefoot* (in Spanish, *in the smith's house, the knife is a stick*).

Second-order/three-way excitation–emission fluorescence data

From the pioneering work in 1978 concerning the quantitative determination of perylene in the presence of interferents by EEFMs and three-way calibration,[22] numerous papers were published on the subject. The most popular model to be applied to EEFM data (which are in principle trilinear) is PARAFAC,[10] which should be the first option for these data. In fact, PARAFAC has been profusely applied to second-order EEFM data for the simultaneous quantitation of fluorescent analytes (or analytes that can be transformed into fluorescent products) in biological, environmental and food samples, among others. PARAFAC is able to overcome the interference cause by both intrinsic and extrinsic fluorescence species potentially present in complex matrices, achieving uniqueness in the data decomposition and thus obtaining the second-order advantage.

There are two general PARAFAC calibrations of EEFM datasets: (1) the experimentally simpler external calibration, which consists of building a calibration set prepared with standard solutions of the analytes, and (2) standard addition, where the analyte standard is added to aliquots of the analyzed sample before reading the data. The latter strategy is experimentally more laborious, but is the alternative to be applied when the so-called matrix effect is corroborated in the system under study. The matrix effect modifies the signal-concentration relation in a sample dependent manner, and thus breaks the trilinearity of EEFM data. In this case, PARAFAC cannot be successfully applied using the usual external calibration procedure. The matrix effect is frequently present in complex biological or environmental samples, and specifically in plasma and urine, where it is usually caused by the quenching action of proteins when they bind to the analyte. Table 1 shows selected examples from recent years of PARAFAC analyte determinations based on EEFM and either external or standard addition calibration.

In the presence of a matrix inner-filter effect, an easier protocol than standard addition is to apply U-PLS/RBL to the resulting non-trilinear EEFM data. In 2006, Piccirilli *et al.* demonstrated the ability of this model to overcome the significant changes produced by the fungicide thiabendazole in both the excitation and emission spectra of the fungicide carbendazim.[23] The poor PARAFAC analytical results were attributed to this inner-filter phenomenon. A subsequent report confirmed that U-PLS/RBL is the most successful model for analyte prediction when EEFMs suffer inner-filter effects[24] on the basis of both simulated and experimental data. The latter included calibration mixtures of the analyte chrysene and the inner-filter producing benzopyrene, and test samples containing the interferent pyrene.

Trilinear models may also fail under conditions of near-identical excitation or emission spectral profiles for sample constituents, either analytes or analytes and interferents. In these cases, degeneracy phenomena may preclude the

Table 1 Selected examples for analytical quantitation using EEFM and PARAFAC

Compound	Action/function	Highlight	Sample	Ref.
External calibration				
Fluphenazine	Antipsychotic	Fluorescent derivative ($KMnO_4$ oxidation)	Urine	25
DEX, QUIN	Antitussive, anticonvulsant (DEX); antimalarial (QUIN)		Plasma and urine	26
BTZ	Herbicide	EEFMs measured on a nylon membrane surface	Stream, canal, underground waters	27
IRI, THAL	Anticancer drugs	Analytes with very different fluorescence quantum yields	Urine	28
E1, E3	Estrogens		Liquid cosmetic	29
AFs, OCH A	Mycotoxins	Solvent methanol : water 75 : 25 (v/v)	Sorghum grains	30
AFs B_2 and G_2	Mycotoxins		Peanuts	31
AF B2[a]	Mycotoxin	Derivatization with bromine	Peanuts	32
CAT, HQ, TRY	Dihydroxybenzenes		Aqueous solution	33
BaP, DBA, BaA, CHRY	Potentially carcinogenic PAHs	Nylon-attached rotating disks	Aqueous solution	34
PHEN, TYR, TRYP	Amino acids		Cell culture; human plasma	35
MAG, HON	Polyphenolic compounds		Herb and plasma	36
VAL, AMB	Antihypertensives	SDS as a fluorescence enhancer	Plasma	37
MG, CV, LG, LV	Antimicrobials and antiparasitics in aquaculture	Dispersive liquid–liquid microextraction (preconcentration)	Grass carp and shrimp	38
MOX, CIPRO	Fluoroquinolones		Urine	39
NP ethoxylate, NAPH sulfonate	Industrial contaminants		Waste water	40
Fe(II) ion	Metal ion	Fe^{2+}/H_2O_2 enhance MoS_2 nanosheet catalytic activity for OPD oxidation to DAPN. EEFMs are read from the MoS_2/OPD/H_2O_2 sensor	Lake water	41
AR, HQ[b]	Tyrosinase inhibitors		Cosmetic products	42
Standard-addition calibration				
Glutathione	Antioxidant	Fluorescent adduct with *o*-phthaldehyde	Plasma	43
t-Resveratrol	Antioxidant		Plasma	44
PRO enantiomers	Beta-blocker	β-CD for chiral recognition	Plasma and urine	45
IBU enantiomers	Antiinflammatory	β-CD for chiral recognition	Plasma and urine	46
CBL, CBZ, NAP	Carbamate pesticides	Quenching minimized by dilution	Lime tree flowers	47

[a] In the presence of AF G2. [b] Resolved with the alternating trilinear decomposition (ATLD) model. Abbreviations: AF, aflatoxin; AMB, amlodipine besylate; ARB, arbutin; BAA, benz[*a*]anthracene; BaP, benzo[*a*]pyrene; BTZ, bentazone; CAT, catechol; CBL, carbaryl; CBZ, carbendazim; CD, cyclodextrin; CHRY, chrysene; CIPRO, ciprofloxacin; CV, crystal violet; DAPN, 2,3-diaminophenazine; DBA, dibenz[*a*,*h*]anthracene; DEX, dextromethorphan; E1, estrone; E3, estriol; HON, honokiol; HQ, hydroquinone; IBU, ibuprofen; IRI, irinotecan; LG, leucomalachite green; LV, leucocrystal violet; MAG, magnolol; MG, malachite green; MoS_2, molybdenum disulfide; MOX, moxifloxacin; NAP, 1-naphthol; NAPH, 2-naphthalene; NP, nonylphenol; OCH, ochratoxin; OPD, *o*-phenylenediamine; PAHs, polycyclic aromatic hydrocarbons; PHEN, L-phenylalanine; PRO, propanolol; QUIN, quinidine; SDS, sodium dodecyl sulfate; THAL, thalidomide; TRY, tryptophan; TYR, tyrosine; VAL, valsartan.

decomposition of the three-way data in physically reasonable profiles. More flexible models can be conveniently applied to these data, namely U-PLS/RBL and MCR-ALS. Table 2 displays selected examples related to this latter topic.

We now discuss in detail two working examples of the determination of fluorescent analytes in the presence of interferents through EEFMs and PARAFAC. A very simple and green method following this strategy was developed for PAH determination in aqueous solution.[34] EEFMs were directly recorded on the nylon surface, after analyte extraction in a rotating Teflon disk system attached to the nylon membrane. The assayed compounds were heavy PAHs of environmental concern, namely benzo[*a*]pyrene, dibenz[*a*,*h*]anthracene, benz[*a*]anthracene and chrysene. They were quantified in the presence of other PAHs selected as potential intereferents. The EEFMs were arranged in a three-way array, which complied with the trilinearity condition, and the chemometric analysis was successfully performed using PARAFAC through external calibration.

On the other hand, PARAFAC with the standard addition method was applied for the determination of enantiomers of propranolol (beta blocker) in human plasma and urine.[45] The method is based on chiral recognition by the formation of inclusion complexes with β-cyclodextrin in the presence of 1-butanol. Standard addition is required due to the individual matrix effect caused by the quenching action of the proteins present in the plasma and urine.[25] See all examples in Tables 1 and 2.[25–61]

Second-order/three-way chromatographic-spectral data

In the chromatographic context, the use of appropriate models has the relevant advantage of mathematically solving incompletely resolved bands, dealing with the presence of interference through the second-order advantage, and with the inherent lack of repeatability in the elution profiles (which becomes the breaking mode).[4] The most applied model for second-order chromatographic data processing is thus MCR-ALS, which has become the standard for these types of

Table 2 Selected examples for analytical quantification using EEFMs and models other than PARAFAC

Compound	Action/function	Highlight	Model	Reason	Sample	Ref.
CBS-X, CXT	Used in the detergent industry		SWATLD; APTLD	Spectral similarity analyte-interference[a]	Laundry powder, agriculture soil, wastewater	48
CBZ	Anticonvulsant, emerging pharmaceutical pollutant	EEPIFMs (UV irradiation in acid medium)	MCR-ALS	Spectral similarity analyte-interference	Tap, underground, river waters	49
CBZ, OFLO, PX	Anticonvulsant (CBZ), fluoroquinilone(OFLO), antiinflammatory (PX)	EEPIFMs (UV irradiation)	U-PLS/RBL	Spectral similarity among analytes	River, underground, tap waters	50
BaA, BfF, BkF, BaP, DBA, Bp, Ip	Potentially carcinogenic PAHs		U-PLS/RBL	Spectral similarity among analytes	Olive and sunflower oils	51
BaA, BfF, BkF, BaP, DBA, Bp, Ip	Potentially carcinogenic PAHs	EEFMs on nylon membranes	U-PLS/RBL	Spectral similarity among analytes	Edible oils	52
BaP, DBA, BAA CHRY, BbF, BkF,	Potentially carcinogenic PAHs	flow-through optosensor	U-PLS/RBL	Spectral similarity analyte-interference	River waters, sludges	53
PY, AN, FL FLU, ACE, PHE	Potentially carcinogenic PAHs		U-PLS/RBL	ACE and FL spectral overlapping, low FL fluorescence	River and reservoir waters	54
GAL	Acetylcholinesterase inhibitor	EEFMs in SDS medium	U-PLS/RBL	Spectral similarity analyte-interference	River, tap, well waters	55
TBZ, FBZ	Fungicides	Flow-through optosensor. EEFMs on C18	U-PLS/RBL	Spectral overlapping and difference of quantum efficiencies	Underground, tap, mineral, river waters	56
ISO, LIN, MONU, RIM	Urea-derivative herbicides	EEPIFMs/HTAC medium	U-PLS/RBL	Photoproducts spectral overlapping	Water and soil samples	57
TBT	Organotin species	EEFMs of its morin complex	MCR-ALS	Excitation profiles of interference and free morin overlap	Tap, river, lagoon, sea waters	58
TBT	Organotin species	EEFMs of TBT-morin complex after CPE	MCR-ALS	Emission overlapping of TBT-morin, free morin and interference	Marine sediments	59
E2	Estrogen	EEFMs on a C18 surface	U-PLS/RBL, MCR-ALS	Analyte-interference spectral similarity	Fish/chicken tissues	60
BPA, NP	Xenoestrogens	CD-enhanced EEFMs	U-PLS/RBL	Analytes spectral similarity	Plastics	61

[a] PARAFAC fails only in wastewater samples. Abbreviations: ACE, acenaphthene; AN, anthracene; APTLD, alternating penalty trilinear decomposition; BaA, benzo[*a*]anthracene; BaP, benzo[*a*]pyrene; BbF, benzo[*b*]fluoranthene; BkF, benzo[*k*]fluoranthene; BP, benzo[*g*,*h*,*i*]perylene; BPA, bisphenol A; CBS-X, benzenesulfonic acid, 2,2′([1,1′-biphenyl]-4,4′-diyldi-2,1-ethenediyl) bis-disodium; CBZ, carbamazepine; CD, cyclodextrin; CHRY, chrysene; CPE, cloud point extraction; CXT, disodium 4,4′-bis[(4-anilino-6-morpholion-1,3,5-trizin-2-yl)amino]stilbene-2,2′-disulphonate; DBA, dibenz[*a*,*h*]anthracene; E2, 17β-estradiol; EEPIFMs, excitation–emission photoinduced fluorescence matrices; FBZ, fuberidazole; FL, fluoranthene; FLU, fluorene; GAL, galantamine; HTAC, hexadecyltrimethylammonium chloride; IP, indeno[1,2,3-*c*,*d*]-pyrene; ISO, isoproturon; LIN, linuron; MONU, monuron; NP, nonylphenol; OFLO, ofloxacin; PAHs, polycyclic aromatic hydrocarbons; PHE, phenanthrene; PX, piroxicam; PY, pyrene; RIM, rimsulfuron; SDS, sodium dodecyl sulfate; SWATLD, self-weighted alternating trilinear decomposition; TBT, tributyltin; TBZ, thiabendazole.

data. Selected examples where second-order liquid chromatographic data were successfully processed with MCR-ALS are shown in Table 3.

Table 4 shows relatively recent examples where liquid chromatography second-order data were successfully processed by other models. As explained above, when trilinear models were applied, chromatographic bands did not significantly change between successive runs, or data were aligned applied before data processing. However, it should be borne in mind that the latter are not the general solutions to the universal problem of lack of chromatographic reproducibility and the presence of interferents. Slight trilinearity losses were also resolved by latent structured RBL models.

Two examples are detailed here. Mancha de Llanos *et al.* reported a typical work showing the advantages of coupling MCR-ALS to HPLC-FLD second-order data aimed at the quantitation of five marker pteridines (neopterin, biopterin, pterin, xanthopterin and isoxanthopterin) in urine samples.[65] A fast-scanning spectrofluorimeter connected to a chromatograph allowed obtaining the data matrices of fluorescence intensity as a function of retention time and emission wavelength. MCR-ALS enabled the determination of the analytes, some of them with severely overlapped profiles, in the presence of coeluting interference, in a short experimental time with low reagent consumption.

Vosough *et al.* compared the performances of MCR-ALS and U-PLS/RBL as applied to HPLC-DAD matrix data, analyzing the prediction results for six antibiotics (amoxicillin, metronidazole, sulfamethoxazole, ofloxacine, sulfadiazine and sulfamerazine) in the sewage treatment plant influent and effluent samples.[69] Although in most cases both models yielded good results, MCR-ALS proved to be more efficient for modeling datasets with elution profile changes from sample to sample,

Table 3 Selected examples for analytical quantification using second-order liquid-chromatographic data and MCR-ALS

Compound	Action/function	Detection	Highlight	Sample	Ref.
BIO, NEO, PT, XAN, ISO	Metabolic disorder markers	FLD		Urine	65
BIO, NEO, PT, XAN, ISO	Metabolic disorder markers	FLD	Augmented in spectra	Urine	66
Daidzein, genistein	Phytoestrogens	DAD		River water	67
MNZ, SMX, CPL, SDZ, SM	Antibiotics	DAD		Wastewaters	68
MNZ, SMX, OFL, SDZ, SM, AMOX[a]	Antibiotics	DAD		Sewage	69
13-*cis*-RA, 9-*cis*-RA, 9,13-di-*cis*-RA	Expression gene regulators during growth	DAD		Plasma	70
E3, E2, EE2, E1	Estrogens	DAD	ET axis divided in regions due to spectral similarities	Tap, mineral, river underground waters	71
E3, E2, E1, EE2, DES, HEX, MEST, PROG, AE NOR, LEV	Sex hormones	DAD-FLD	Dual detection in single isocratic runs	Mineral, river, underground waters. Sediments	72
ENO, NRF, OFL, SRF, CPF, DIF, EN	Fluoroquinolones	FLD	Fluorescence enhancement by addition of yttrium	Stream, waste, well waters	73
PHENO, CAR	Antiepileptics	DAD		Human serum	74
PPX, CBL, CBZ, TBZ, FBZ	Pesticides	DAD		Fruits, juices	75
BPA, NP, OP, DBP, DEHP, DEP	Endocrine-disruptors	DAD-FLD	Dual detection. Elution gradient for shortening the run time: 14 min per sample	Beer, wine, soda, juice, water, distilled beverages	76
ALDSX, OXA, ALDSN, MET, 3HOC, ALD, PPX, CBF, CBL, NAP, METH	Pesticides	DAD		River water	77
SOT, ATE, NAD, PIN, METR, TIM, BIS, PRO, BE, PARA, PHEN	Beta-blockers and analgesics (PARA, PHEN)	DAD	Precolumn replaced by a short C18 column allowing preconcentration/clean-up	River water	78
METHAM, PSEPHE	Central nervous system stimulants	DAD		Ground[b], river[c] waters	79
GAL, EPI-GAL, OD-GAL, ND-GAL, NO-GAL	Cholinesterase inhibitor (GAL) and its metabolites	FLD	ET axis divided in regions due to spectral similarities	Serum	80
TRY, PHE, PUT, CAD, HIS	Biogenic amines	DAD	Derivatization. Alignment before MCR-ALS augmented in spectra	Fish	81
TBZ, FBZ, CBZ, FM, DICAM, IMZQ, NFZ, CBL, METH, NAP	Agrochemicals	DAD-FLD	Dual detection. FLD-ET data at two excitation wavelengths	Mushroom, lettuce, alfalfa sprout, cucumber, celery	82
SYR, VAN, PABA, CAF[d]	Antioxidant phenolics	DAD		Olive oils	83
TMP, EN, IMD, CLB,DIF, CFT, CPL, CTC, FLUM, PSL, PYRA, MBT, ABZ, FXN, DZP, FEN, NIC, IBU, DICL, BMV, PROG	Veterinary active ingredients	DAD-FLD	Optimization through experimental design for improving the analyte extraction efficiency	Poultry litter	84
DMP, CBL, BPA, NAP, NFZ	Endocrine disruptors	Fused DAD-FLD data	Analytes that cannot be quantified from individual detectors. High selectivity	Tap, underground, river waters	85

[a] MCR-ALS and U-PLS/RBL rendered comparable results. [b] External calibration method. [c] Standard addition method. [d] MCR-ALS and PARAFAC2 (MCR provided significantly better results both in terms of modeling and predictive ability). Abbreviations: ABZ, albendazole; AE, androstenedione; ALD, aldicarb; ALDSX, aldicarb sulfoxide; ALDSN, aldicarb sulfone; AMOX, amoxicillin; ATE, atenolol; BE, betaxolol; BIO, biopterin; BIS, bisoprolol; BMV, betamethasone; BPA, bisphenol A; CAD, cadaverine; CAF, caffeic acid; CAR, carbamazepine; CBF, carbofuran; CBL, carbaryl; CBZ, carbendazim; CFT, ceftiofur; CLB, clenbuterol; CPF, ciprofloxacin; CPL, chloramphenicol; CTC, chlortetracycline; DBP, dibutyl phthalate; DEHP, diethylhexyl phthalate; DEP, diethyl phthalate; DES, diethylstilbestrol; DICAM, dicamba; DICL, diclofenac; DIF, difloxacin; DMP, dimethyl phthalate; DZP, diazepam; E1, estrone; E2, 17β-estradiol; E3, estriol; EE2, 17α-ethynylestradiol; EN, enrofloxacin; ENO, enoxacin; EPI-GAL, epigalantamine; ET, elution time; FBZ, fuberidazole; FEN, fenbendazole; FLUM, flumequine; FM, fenarimol, FXN, flunixin; GAL, galantamine; HEX, hexestrol; HIS, histamine; 3HOC, 3-hydroxy-carbofuran; IBU, ibuprofen; IMZQ, imazaquin; IMD, imidacloprid; ISO, isoxanthopterin; LEV, levonorgestrel; MBT, menbutone; MEST, mestranol; MET, methomyl; METH, methiocarb; METHAM, methamphetamine; METR, metoprolol; MNZ, metronidazole; NAD, nadolol; NAP, 1-naphthol; NEO, neopterin; ND-GAL, *N*-demethylgalantamine; NFZ, norflurazon; NIC, nicarbazin; NO-GAL, galantamine *N*-oxide; NOR, norethisterone; NP, nonylphenol; NRF, norfloxacin; OD-GAL; *O*-demethylgalantamine; OFL, ofloxacin; OP, octylphenol; OXA, oxamyl; PABA, *p*-hydroxybenzoic acid; PARA, paracetamol; PHE, 2-phenylethylamine; PHEN, phenazone; PHENO, phenobarbital; PIN, pindolol; PSL, prednisolone; PPX, propoxur; PRO, propanolol; PROG, progesterone; PSEPHE, pseudoephedrine; PT, pterin; PUT, putrescine; PYRA, pyrantel; 9-*cis*-RA, 9-*cis*-retinoic acid; 13-*cis*-RA, 13-*cis*-retinoic acid; 9,13-di-*cis*-RA, 9,13-di-*cis*-retinoic acid; SDZ, sulfadiazine; SM, sulfamerazine; SMX, sulfamethoxazole; SOT, sotalol; SRF, sarafloxacin; SYR, syringic acid; TBZ, thiabendazole; TIM, timolol; TMP, trimethoprim; TRY, tryptamine; VAN, vanillic acid; XAN, xanthopterin.

whereas U-PLS/RBL appeared to be better for components with high spectral similarity.

In the cases where the analytes have very similar UV or fluorescence profiles, *e.g.* estrogens and some sex hormones, a wise alternative is to divide the time axis in different regions for data processing, each one including a single analyte.[71,72] It is also important to highlight the ability of MCR-ALS to successfully process fused second-order chromatographic data.[85]

Table 4 Selected examples for analytical quantifications using second-order liquid-chromatographic data and models other than MCR-ALS

Compound	Action/function	Detection	Model	Sample	Ref.
AFs B1, B2, G1 and G2		DAD	PARAFAC	Pistachio nuts	86
ATR, AME, PROM	Herbicides	DAD	APTLD	River sediment, wastewaters	87
Twenty free amino acids	Amino acids influence the flavor of tea	FLD	APTLD	Tea infusions	88
PROM, NAPRO, ALA	Herbicides	DAD	SWATLD	River sediment, wastewaters	89
CIPRO, DAN, DIF, ENO, ENR, FLE, LOM, MAR, OFLO, ORB, PEF, SAR	Quinolones (antibiotics)	DAD	ATLD	Honey	90
PG, TBHQ, NDGA, EQ, BHA, OG, DG, Ionox-100, BHT	Synthetic phenolic antioxidants	DAD	APTLD	Oil samples	91
PG, BHA, BHT, OG, TBHQ, DG, NDGA	Synthetic phenolic antioxidants	FLD	ATLD	Oil samples	92
SC, SM, SMX, PIP, PEF, DAN, LOM, TC, MNZ, ORN, OTC	Antibiotics	DAD	PARAFAC[a]	Tap waters	93
RU, QUE, LUT, KAE, ISOR, API, GALA, CHRYS	Flavonoids	DAD	ATLD	Propolis capsules	94
ISO, MONU, RIM	Urea-derivative herbicides	PIF	U-PLS/RBL[b]	Tap, river, underground waters	95
CAR, NX, DICL, GEM, MEF	Pharmaceuticals (emerging pollutants)	DAD	(1) COW alignment and PARAFAC. (2) MCR-ALS with trilinearity constraint[c]	Well, river waters	96

[a] Chromatographic background drift correction using a strategy based on orthogonal spectral signal projection. [b] Post-column photoirradiation. [c] Similar results were obtained with both procedures. Abbreviations: AF, aflatoxin; ALA, alachlor; AME, ametryn; API, apigenin; APTLD, alternating penalty trilinear decomposition; ATLD, alternating trilinear decomposition; ATR, atrazine; BHA, 3-*tert*-butyl-4-hydroxyanisole; BHT, 3,5-di-*tert*-butyl-4-hydroxytoluene; CAR, carbamazepine; CHRYS, chrysin; CIPRO, ciprofloxacin; COW, correlation optimized warping; DAD, diode-array detector; DAN, danofloxacin; DICL, diclofenac; DIF, difloxacin; ENO, enoxacin; ENR, enrofloxacin; DG, dodecyl gallate; EQ, ethoxyquin; FLD, fluorescence detector; FLE, fleroxacin; GALA, galangin; Ionox-1002, 6-di-*tert*-butyl-4-hydroxymethyphenol; GEM, gemfibrozil; ISO, isoproturon; ISOR, isorhamnetin; KAE, kaempferol; LOM, lomefloxacin; LUT, luteolin; MAR, marbofloxacin; MEF, mefenamic acid; MNZ, metronidazole; MONU, monuron; NAPRO, napropamide; NDGA, nordihydroguaiaretic acid; NX, naproxen; OFLO, ofloxacin; OG, octyl gallate; ORB, orbfloxacin; ORN, ornidazole; OTC, oxytetracycline; PEF, pefloxacin; PG, propyl gallate; PIP, pipemidic acid; PROM, prometryne; QUE, quercetin; RIM, rimsulfuron; RU, rutin; SAR, sarafloxacin; SC, sulfacetamide; SM, sulfamerazine; SMX, sulfamethoxazole; SWATLD, self-weighted alternating trilinear decomposition; TC, tetracycline; THBP, 2,4,5-trihydroxybutyrophenone; TBHQ, *tert*-butylhydroquinone.

Data fusion is useful when analytes cannot be quantitated from individual detectors and enhances the advantages already achieved with the coupling of dual chromatographic detection to multivariate calibration.

In general, liquid or gas chromatography with mass spectral detection provides enough selectivity to successfully determine individual analytes in mixtures, with no need for three-way calibration assistance. However, highly complex samples or analytes with very similar structures may require the use of chemometrics. Pertinent examples include the analysis of nearly co-eluting ^{12}C and ^{13}C isotopically labeled metabolites by GC-MS data, which were first aligned and then processed with PARAFAC,[62] polycyclic aromatic hydrocarbons in water samples by GC-MS and MCR-ALS,[63] and amphetamines in bacterial lipid extracts by LC-MS data and MCR-ALS.[64] See all examples in Tables 3 and 4.[64–96]

Third-order/four-way data

Although third-order data can be generated by different strategies, the most applied ones include the measurement of: (1) EEFMs as a function of either reaction time or chromatographic elution time, and (2) comprehensive two-dimensional chromatography with spectral detection. If the data are quadrilinear, four-way PARAFAC is the option to be applied for data processing, with small deviations from quadrilinearity resolved with more flexible PLS-RTL models. This is the case with non-chromatographic third-order data (EEFM-reaction time), whose examples are shown in Table 5 for the determination of pollutants and compounds with biological activity.

Few studies have been reported introducing an additional mode to EEFMs, other than the reaction time. One example is the pH mode, introduced by collecting EEFMs with a fast-scanning spectrofluorimeter at the output of a flow injection system where a double pH gradient was created.[97] In this case, four-way PARAFAC was successfully employed to quantitate fluoroquinolone antibiotics in human urine following this protocol.

Other alternatives to create the additional data mode in EEFM detection include: (1) variations in dilution factors, as in the quantitation of the pollutants carbaryl, carbendazim and 1-naphthol in iceberg lettuce,[98] (2) solvent changes, as in the detection of schizandrols A and B (active ingredients of anti-free radical and anti-HIV *Schisandra chinensis*) in Dulbecco's modified Eagle's medium samples,[99] and in the quantitation of aflatoxins B_1 and B_2 in peanuts.[100] All of these systems were successfully resolved using PARAFAC.

On the other hand, chromatographic systems call for the application of non-quadrilinear models because of the occurrence of one or two breaking modes: the elution time mode(s). Liquid chromatographic data with EEFM detection have a single breaking mode (the elution time mode) and can be pro-

Table 5 Selected examples of third-order data including EEFM measurements

Analyte	Action/function	Highlight	Model	Sample	Ref.
EEFM-kinetic third-order data					
TYR, LEV	Dopamine precursors	Reaction involved: enzyme-induced	AQLD	Human plasma	101
BaP, DBA, BbF, BkF, BAA	PAHs	Reaction involved: Fenton degradation	PARAFAC	Natural waters	102
Thiamine	Vitamin B1	Reaction involved: oxidation in alkaline medium catalyzed by Hg^{2+}	PARAFAC	Multivitamin complexes	103
AZM		Reaction involved: UV-light irradiation	PARAFAC and U-PLS/RTL[a]	Fruits	104
CBL, NAP, PPX	Pesticides	Reaction involved: alkaline hydrolysis of the pesticides	U-PLS/RTL and N-PLS/RTL	Natural water stream	105
EEFM-liquid chromatography third-order data					
Chl *a*, Chl *b*, Pheo *a*, Pheo *b*	Natural pigments of virgin olive oil	ETMs recorded at different excitation wavelengths (the same sample is injected several times)	U-PLS/RTL and N-PLS/RTL	Olive oils	106
Chl *a*, Chl *b*, Pheo *a*, Pheo *b*	Natural pigments of virgin olive oil	ETMs recorded at different excitation wavelengths (the same sample is injected several times)	Augmented PARAFAC	Olive oils	18
OFL, CIPRO	Fluoroquinolones	EEFMs at different elution times[b]	MCR-ALS	Tap water	107
OFL, CIPRO, DAN	Fluoroquinolones	EEFMs at different elution times[b]	Augmented PARAFAC	Drinking water samples	108
CBZ, TBZ, FBZ, CBF, CBL, NAP	Pesticides	Each sample is injected several times, and ETMs are recorded each time at a different excitation wavelength	U-PLS/RTL	Fruit juice	109

[a] Both models rendered good results. [b] At the end of the chromatographic procedure, each fraction is collected in an ELISA (enzyme-linked immunosorbent assay) 96-well plate (several fractions are collected for each run). Abbreviations: AQLD, alternating quadrilinear decomposition; AZM, azinphos-methyl; BAA, benz[*a*]anthracene; BaP, benzo[*a*]pyrene; BbF, benzo[*b*]fluoranthene; BkF, benzo[*k*]fluoranthene; CBF, carbofuran; CBL, carbaryl; CBZ, carbendazim; Chl, chlorophyll; CIPRO, ciprofloxacin; DAN, danofloxacin; DBA, dibenz[*a*,*h*]anthracene; EEFM, excitation–emission fluorescence matrix; ETM, emission wavelength–elution time matrix; FBZ, fuberidazole; LEV, levodopa; NAP, 1-naphthol; OFL, ofloxacin; Pheo, pheophytin; PPX, propoxur; TBZ, thiabendazole; TYR, tyrosine.

Table 6 Selected examples of two-dimensional chromatographic third-order data

Analyte	Action/function	Highlight	Model	Sample	Ref.
GC-GC-MS third-order data					
PAHs	Pollutants		MCR-ALS	North Sea crude oil extract	110
PAHs	Pollutants		MCR-ALS	Heavy fuel oils	111
LC-LC-DAD third-order data					
Furanocoumarins	Pollutants		MCR-ALS	Apiaceous vegetables	112
Phenytoin	Pollutant	Semi-automated peak alignment to restore quadrilinearity	PARAFAC	Waste waters	113
Nitrate, TRY, OH-TRY, IAc, IPr, Ian, TYR	Metabolites and xenobiotics		MCR-ALS	Human urine	114

IAc, indole-3-acetic acid; IAn, indole-3-acetonitrile; IPr, indole-3-propionic acid; OH-TRY, hydroxytryptophan; PAHs, polycyclic aromatic hydrocarbons; TRY, tryptophan; TYR, tyrosine.

cessed by three-way augmented PARAFAC. In cases of no significant peak changes and high collinearity among spectra, however, PLS/RTL gave the best results. Examples of such systems, resolved by different models, are summarized in Table 5.

Finally, an important group of third-order applications includes two-dimensional liquid chromatography with a diode array detector (DAD) or MS detection and gas chromatography with mass spectral detection (GC-GC-MS). Changes in profiles from sample to sample in both columns make it necessary to process the data by building a super-augmented matrix with sample data which are previously unfolded by concatenating both elution time modes. Two breaking modes are present in these systems, and the model of choice for decomposing the bilinear super-augmented matrix is MCR-ALS. In some cases alignment in both time modes may be possible, recovering quadrilinearity before PARAFAC processing. We collect selected examples in Table 6.

Conclusions

With the expansion of the multi-way calibration field to new multi-dimensional signals and analytical systems, there is a need for a rational scheme to aid the analyst in selecting the most appropriate model for successful data processing. The present review provides one such alternative, based on a simple analysis of two relevant data properties: (1) the number

of modes which break the multi-linearity due to sample-dependent profile changes, and (2) the number of mutually dependent instrumental modes. The importance of model selection cannot be overemphasized: it is the first step towards the success of any multi-way calibration protocol.

Acknowledgements

The authors wish to acknowledge the financial support from Universidad Nacional de Rosario, CONICET (Consejo Nacional de Investigaciones Científicas y Técnicas, Project No. PIP 0163) and ANPCyT (Agencia Nacional de Promoción Científica y Tecnológica, Project No. PICT-2013-0136).

References

1 A. C. Olivieri and G. M. Escandar, *Practical three-way calibration*, Elsevier, Waltham, USA, 2014.
2 *Data Handling in Science and Technology, Vol. 29, Fundamentals and analytical applications of multiway calibration*, ed. A. Muñoz de la Peña, H. C. Goicoechea, G. M. Escandar and A. C. Olivieri, Elsevier, Amsterdam, 2015.
3 K. S. Booksh and B. R. Kowalski, *Anal. Chem.*, 1994, **66**, 782A–791A.
4 A. C. Olivieri, *Anal. Methods*, 2010, **4**, 1876–1886.
5 J. A. Arancibia, P. C. Damiani, G. M. Escandar, G. A. Ibañez and A. C. Olivieri, *J. Chromatogr. B: Biomed. Appl.*, 2012, **910**, 22–30.
6 A. C. Olivieri, *Chem. Rev.*, 2014, **114**, 5358–5378.
7 G. M. Escandar, H. C. Goicoechea, A. Muñoz de la Peña and A. C. Olivieri, *Anal. Chim. Acta*, 2014, **806**, 8–26.
8 H. Parastar and R. Tauler, *Anal. Chem.*, 2014, **86**, 286–297.
9 A. R. Jalalvand, H. C. Goicoechea and D. N. Rutledge, *Trends Anal. Chem.*, 2017, **87**, 32–48.
10 R. Bro, *Chemom. Intell. Lab. Syst.*, 1997, **38**, 149–171.
11 R. Tauler, M. Maeder and A. de Juan, Multiset data analysis: extended multivariate curve resolution, in *Comprehensive chemometrics*, ed. S. Brown, R. Tauler and B. Walczak, Elsevier, Oxford, UK, 2009, pp. 473–505.
12 B. E. Wilson, W. Lindberg and B. R. Kowalski, *J. Am. Chem. Soc.*, 1989, **111**, 3797–3804.
13 C. G. Zampronio, S. P. Gurden, L. A. Moraes, M. N. Eberlin, A. K. Smilde and R. J. Poppi, *Analyst*, 2002, **127**, 1054–1060.
14 K. Calimag-Williams, G. Knobel, H. C. Goicoechea and A. D. Campiglia, *Anal. Chim. Acta*, 2014, **811**, 60–69.
15 S. A. Bortolato, V. A. Lozano, A. Muñoz de la Peña and A. C. Olivieri, *Chemom. Intell. Lab. Syst.*, 2015, **141**, 1–11.
16 J. A. Arancibia, A. C. Olivieri, D. Bohoyo Gil, A. Espinosa Mansilla, I. Durán Merás and A. Muñoz de la Peña, *Chemom. Intell. Lab. Syst.*, 2006, **80**, 77–86.
17 R. M. Maggio, A. Muñoz de la Peña and A. C. Olivieri, *Chemom. Intell. Lab. Syst.*, 2011, **109**, 178–185.
18 X. D. Qing, H. L. Wu, X. H. Zhang, Y. Li, H. W. Gu and R. Q. Yu, *Anal. Chim. Acta*, 2015, **861**, 12–24.
19 J. Öhman, P. Geladi and W. Wold, *J. Chemom.*, 1990, **4**, 79–90.
20 H. A. L. Kiers, J. M. F. Ten Berge and R. Bro, *J. Chemom.*, 1999, **13**, 275–294.
21 S. A. Bortolato and A. C. Olivieri, *Anal. Chim. Acta*, 2014, **842**, 11–19.
22 C. N. Ho, G. D. Christian and E. R. Davidson, *Anal. Chem.*, 1978, **50**, 1108–1113.
23 G. N. Piccirilli and G. M. Escandar, *Analyst*, 2006, **131**, 1012–1020.
24 D. Bohoyo Gil, A. Muñoz de la Peña, J. A. Arancibia, G. M. Escandar and A. C. Olivieri, *Anal. Chem.*, 2006, **78**, 8051–8058.
25 S. F. Li, H. L. Wu, L. Huang, Y. N. Li, J. F. Nie, S. R. Zhang and R. Q. Yu, *Anal. Methods*, 2010, **2**, 1069–1077.
26 H. Y. Zou, H. L. Wu, Y. N. Li, J. F. Nie, H. Y. Fu, S. F. Li and R. Q. Yu, *Anal. Lett.*, 2010, **43**, 2739–2750.
27 J. P. Chiarandini and G. M. Escandar, *Anal. Bioanal. Chem.*, 2012, **402**, 2221–2225.
28 M. C. Hurtado-Sánchez, I. Durán-Merás, M. I. Rodríguez-Cáceres, A. Jiménez-Girón and A. C. Olivieri, *Talanta*, 2012, **88**, 609–616.
29 D. Z. Tu, H. L. Wu, Y. N. Li, J. Zhang, Y. Li, C. C. Nie, X. H. Zhang and R. Q. Yu, *Anal. Methods*, 2012, **4**, 222–229.
30 M. C. Rodríguez, G. H. Sánchez, M. S. Sobrero, A. V. Schenone and N. R. Marsili, *Microchem. J.*, 2013, **110**, 480–484.
31 A. S. Luna, R. A. Luiz, I. C. A. Lima, P. H. Março, P. Valderrama, R. Boqué and J. Ferré, *Anal. Chim. Acta*, 2013, **778**, 9–14.
32 A. S. Luna, I. C. A. Lima, R. L. Alves, W. F. Rocha, R. Boqué and J. Ferré, *Am. J. Quantum Spectrosc.*, 2015, **2**, 1–13.
33 H. Chen, Z. Lin, H. Tang, T. Wu and C. Tan, *J. Spectrosc.*, 2014, **2014**, DOI: 10.1155/2014/412039.
34 A. Cañas, P. Richter and G. M. Escandar, *Anal. Chim. Acta*, 2014, **852**, 105–111.
35 C. Kang, H. L. Wu, S. X. Xiang, L. X. Xie, Y. J. Liu, Y. J. Yu, J. J. Sun and R. Q. Yu, *Anal. Methods*, 2014, **6**, 6358–6368.
36 L. Hu and C. Yin, *Anal. Methods*, 2015, **7**, 5913–5923.
37 H. Y. Fu, H. D. Li, C. Ni, T. M. Yang, Y. Fan, H. Zhang, J. Yang, L. Chen and Y. B. She, *J. Spectrosc.*, 2015, **2015**, DOI: 10.1155/2015/681320.
38 S. Ju, J. Deng, J. Cheng, N. Xiao, K. Huang, C. Hu, H. Zhao, J. Xie and X. Zhan, *Food Chem.*, 2015, **185**, 479–487.
39 M. Vosough, S. N. Eshlaghi and R. Zadmard, *Spectrochim. Acta, Part A*, 2015, **136**, 618–624.
40 A. Mohsenikia, A. Gholami, S. Masoum and S. Abbasi, *Environ. Technol.*, 2016, DOI: 10.1080/09593330.2016.1256437.
41 J. Hu, Q. Zhuang, Y. Wang and Y. Ni, *Analyst*, 2016, **141**, 1822–1829.

42 L. Zhu, H. L. Wu, L. X. Xie, H. Fang, S. X. Xiang, Y. Hu, Z. Liu, T. Wang and R. Q. Yu, *Anal. Methods*, 2016, **8**, 4941–4948.
43 B. Hemmateenejad, Z. Rezaei and S. Zaeri, *Talanta*, 2009, **79**, 648–656.
44 C. D. Bernardes, R. J. Poppi and M. M. Sena, *Talanta*, 2010, **82**, 640–645.
45 P. Valderrama and R. J. Poppi, *Anal. Chim. Acta*, 2009, **651**, 31–35.
46 P. Valderrama and R. J. Poppi, *Chemom. Intell. Lab. Syst.*, 2011, **106**, 160–165.
47 L. Rubio Martínez, M. C. Ortiz Fernández and L. A. Sarabia Peinador, *Anal. Chim. Acta*, 2014, **820**, 9–22.
48 A. Gholami, S. Masoum, A. Mohsenikia and S. Abbasi, *Spectrochim. Acta, Part A*, 2016, **153**, 108–117.
49 V. A. Lozano and G. M. Escandar, *Anal. Chim. Acta*, 2013, **782**, 37–45.
50 M. C. Hurtado-Sánchez, V. A. Lozano, M. I. Rodríguez-Cáceres, I. Durán-Merás and G. M. Escandar, *Talanta*, 2015, **134**, 215–223.
51 F. Alarcón, M. E. Báez, M. Bravo, P. Richter, G. M. Escandar, A. C. Olivieri and E. Fuentes, *Talanta*, 2013, **103**, 361–370.
52 V. Vásquez, M. E. Báez, M. Bravo and E. Fuentes, *Anal. Bioanal. Chem.*, 2013, **405**, 7497–7507.
53 S. A. Bortolato, J. A. Arancibia and G. M. Escandar, *Environ. Sci. Technol.*, 2011, **45**, 1513–1520.
54 R. Yang, N. Zhao, X. Xiao, G. Yin, S. Yu, J. Liu and W. Liu, *Opt. Express*, 2016, **24**, A1148–A1157.
55 M. J. Culzoni, R. Q. Aucelio and G. M. Escandar, *Talanta*, 2010, **82**, 325–332.
56 G. N. Piccirilli and G. M. Escandar, *Analyst*, 2010, **135**, 1299–1308.
57 V. A. Lozano and G. M. Escandar, *Anal. Methods*, 2016, **8**, 7396–7404.
58 M. Bravo, L. F. Aguilar, W. Quiroz, A. C. Olivieri and G. M. Escandar, *Microchem. J.*, 2013, **106**, 95–101.
59 F. Alarcón, R. Bustamante, W. Quiroz, L. F. Aguilar and M. A. Bravo, *Microchem. J.*, 2016, **124**, 132–138.
60 R. L. Pérez and G. M. Escandar, *Microchem. J.*, 2015, **118**, 141–149.
61 R. B. Pellegrino Vidal, G. A. Ibañez and G. M. Escandar, *Talanta*, 2015, **143**, 162–168.
62 S. Yang, J. S. Nadeau, E. M. Humston-Fulmer, J. C. Hoggard, M. E. Lidstrom and R. E. Synovec, *J. Chromatogr. A*, 2012, **1240**, 156–164.
63 M. Ahmadvand, H. Sereshti and H. Parastar, *J. Chromatogr. A*, 2015, **1413**, 117–126.
64 M. M. Sinanian, D. W. Cook, S. C. Rutan and D. S. Wijesinghe, *Anal. Chem.*, 2016, **88**, 11092–11099.
65 A. Mancha de Llanos, M. M. De Zan, M. J. Culzoni, A. Espinosa-Mansilla, F. Cañada-Cañada, A. Muñoz de la Peña and H. C. Goicoechea, *Anal. Bioanal. Chem.*, 2011, **399**, 2123–2135.
66 M. J. Culzoni, A. Mancha de Llanos, M. M. De Zan, A. Espinosa-Mansilla, F. Cañada-Cañada, A. Muñoz de la Peña and H. C. Goicoechea, *Talanta*, 2011, **85**, 2368–2374.
67 E. D. T. Moreira, L. Pinto, A. A. Gomes, H. C. Goicoechea and M. C. Ugulino de Araújo, *J. Braz. Chem. Soc.*, 2015, **26**, 1573–1582.
68 M. Vosough and H. M. Esfahani, *Talanta*, 2013, **113**, 68–75.
69 M. Vosough, M. Rashvand, H. M. Esfahani, K. Kargosha and A. Salemi, *Talanta*, 2015, **135**, 7–17.
70 C. M. Teglia, M. S. Cámara and H. C. Goicoechea, *Anal. Bioanal. Chem.*, 2014, **406**, 7989–7998.
71 R. L. Pérez and G. M. Escandar, *Anal. Chim. Acta*, 2014, **835**, 19–28.
72 R. L. Pérez and G. M. Escandar, *Environ. Pollut.*, 2016, **209**, 114–122.
73 M. R. Alcaráz, M. J. Culzoni and H. C. Goicoechea, *Anal. Chim. Acta*, 2016, **902**, 50–58.
74 M. Vosough, S. Ghafghazi and M. Sabetkasaei, *Talanta*, 2014, **119**, 17–23.
75 V. Boeris, J. A. Arancibia and A. C. Olivieri, *Anal. Chim. Acta*, 2014, **814**, 23–30.
76 R. B. Pellegrino Vidal, G. A. Ibañez and G. M. Escandar, *Talanta*, 2016, **159**, 336–343.
77 R. M. Maggio, P. C. Damiani and A. C. Olivieri, *Talanta*, 2011, **83**, 1173–1180.
78 M. Martínez Galera, M. D. Gil García, M. J. Culzoni and H. C. Goicoechea, *J. Chromatogr. A*, 2010, **1217**, 2042–2049.
79 M. Vosough, H. Mohamedian, A. Salemi and T. Baheri, *J. Chromatogr. Sci.*, 2015, **53**, 233–239.
80 M. J. Culzoni, R. Q. Aucelio and G. M. Escandar, *Anal. Chim. Acta*, 2012, **740**, 27–35.
81 L. Pinto, C. H. Díaz Nieto, M. A. Zon, H. Fernández and M. C. Ugulino de Araújo, *Anal. Chim. Acta*, 2016, **902**, 59–69.
82 M. D. Carabajal, J. A. Arancibia and G. M. Escandar, *Microchem. J.*, 2016, **128**, 34–41.
83 F. Marini, A. D'Aloise, R. Bucci, F. Buiarelli, A. L. Magrì and A. D. Magrì, *Chemom. Intell. Lab. Syst.*, 2011, **106**, 142–149.
84 C. M. Teglia, P. M. Peltzer, S. N. Seib, R. C. Lajmanovich, M. J. Culzoni and H. C. Goicoechea, *Talanta*, 2017, **167**, 442–452.
85 R. B. Pellegrino Vidal, G. A. Ibañez and G. M. Escandar, *Anal. Chem.*, 2017, **89**, 3029–3035.
86 M. Vosough, M. Bayat and A. Salemi, *Anal. Chim. Acta*, 2010, **663**, 11–18.
87 Y. N. Li, H. L. Wu, X. D. Qing, Q. Li, S. F. Li, H. Y. Fu, Y. J. Yu and R. Q. Yu, *Anal. Chim. Acta*, 2010, **678**, 26–33.
88 F. Tan, C. Tan, A. Zhao and M. Li, *J. Agric. Food Chem.*, 2011, **59**, 10839–10847.
89 X. D. Qing, H. L. Wu, Y. N. Li, C. C. Nie, J. Y. Wang, S. H. Zhu and R. Q. Yu, *Anal. Methods*, 2012, **4**, 685–692.
90 Y. J. Yu, H. L. Wu, S. Z. Shao, C. Kang, J. Zhao, Y. Wang, S. H. Zhu and R. Q. Yu, *Talanta*, 2011, **85**, 1549–1559.
91 J. Y. Wang, H. L. Wu, Y. Chen, Y. M. Sun, Y. J. Yu, X. H. Zhang and R. Q. Yu, *J. Chromatogr. A*, 2012, **1264**, 63–71.
92 J. Y. Wang, H. L. Wu, Y. M. Sun, H. W. Gu, Z. Liu, Y. J. Liu and R. Q. Yu, *J. Chromatogr. B: Biomed. Appl.*, 2014, **947–948**, 32–40.

93 Y. J. Yu, H. L. Wu, H. Y. Fu, J. Zhao, Y. N. Li, S. F. Li, C. Kang and R. Q. Yu, *J. Chromatogr. A*, 2013, **1302**, 72–80.

94 Y. M. Sun, H. L. Wu, J. Y. Wang, Z. Liu, M. Zhai and R. Q. Yu, *J. Chromatogr. B: Biomed. Appl.*, 2014, **962**, 59–67.

95 J. A. Arancibia and G. M. Escandar, *Anal. Methods*, 2014, **6**, 5503–5511.

96 N. Akvan and H. Parastar, *Chemom. Intell. Lab. Syst.*, 2014, **137**, 146–154.

97 A. Pagani and G. A. Ibañez, *Microchem. J.*, 2017, **132**, 211–218.

98 L. Rubio, L. A. Sarabia and M. C. Ortiz, *Talanta*, 2015, **138**, 86–99.

99 X. H. Zhang, H. L. Wu, X. L. Yin, Y. Li, X. D. Qing, H. W. Gu, C. Kang and R. Q. Yu, *Chemom. Intell. Lab. Syst.*, 2016, **155**, 46–53.

100 S. M. Sajjadi, H. Abdollahi, R. Rahmanian and L. Bagheri, *Spectrochim. Acta, Part A*, 2016, **156**, 63–69.

101 L. X. Xie, H. L. Wu, Y. Fang, C. Kang, S. X. Xiang, L. Zhu, X. L. Yin, H. W. Gu, Z. Liu and R. Q. Yu, *Chemom. Intell. Lab. Syst.*, 2015, **148**, 9–19.

102 M. D. Carabajal, J. A. Arancibia and G. M. Escandar, *Talanta*, 2017, **165**, 52–63.

103 W. D. Fragoso and A. C. Olivieri, *Microchem. J.*, 2016, **128**, 42–46.

104 M. Montemurro, G. G. Siano, M. J. Culzoni and H. C. Goicoechea, *Sens. Actuators, B*, 2017, **239**, 397–404.

105 P. Santa Cruz and A. García Reiriz, *Talanta*, 2014, **128**, 450–459.

106 V. A. Lozano, A. Muñoz de la Peña, I. Durán Merás, A. Espinosa Mansilla and G. M. Escandar, *Chemom. Intell. Lab. Syst.*, 2013, **125**, 121–131.

107 M. R. Alcaráz, G. G. Siano, M. J. Culzoni, A. Muñoz de la Peña and H. C. Goicoechea, *Anal. Chim. Acta*, 2014, **809**, 37–46.

108 M. R. Alcaráz, S. A. Bortolato, H. C. Goicoechea and A. C. Olivieri, *Anal. Bioanal. Chem.*, 2015, **407**, 1999–2011.

109 M. Montemurro, L. Pinto, G. Véras, A. de Araújo Gomes, M. J. Culzoni, M. C. Ugulino de Araújo and H. C. Goicoechea, *Talanta*, 2016, **154**, 208–218.

110 H. Parastar, J. R. Radović, J. M. Bayona and R. Tauler, *Anal. Bioanal. Chem.*, 2013, **405**, 6235–6249.

111 H. Parastar, J. R. Radović, M. Jalali-Heravi, S. Diez, J. M. Bayona and R. Tauler, *Anal. Chem.*, 2011, **83**, 9289–9297.

112 E. D. Larson, S. R. Groskreutz, D. C. Harmes, I. C. Gibbs-Hall, S. P. Trudo, R. C. Allen, S. C. Rutan and D. R. Stoll, *Anal. Bioanal. Chem.*, 2013, **405**, 4639–4653.

113 R. C. Allen and S. C. Rutan, *Anal. Chim. Acta*, 2012, **723**, 7–17.

114 H. P. Bailey and S. C. Rutan, *Chemom. Intell. Lab. Syst.*, 2011, **106**, 131–141.